

OPTICAL NAVIGATION FOR AUTONOMOUS APPROACH OF SMALL UNKNOWN BODIES

Jacopo Villa[♦], Saptarshi Bandyopadhyay^{*}, Benjamin Morrell^{*}, Benjamin Hockman^{*}, Shyamkumar Bhaskaran^{*}, Issa Nesnas^{*}; ^{*}Jet Propulsion Laboratory – California Institute of Technology, [♦] KTH – Royal Institute of Technology.

Abstract. *State-of-the-practice navigation toward small unknown celestial bodies heavily relies on ground support, in particular, for optical-based operations such as optical navigation and mapping. In this work, we present a strategy to estimate the Small Body shape, kinematics, and ultimately the spacecraft relative trajectory and associated uncertainties during the approach phase using an autonomous operations pipeline. The estimation starts as early as the body is visible in the camera field of view. Our method makes use of image processing algorithms, together with the JPL Mission Analysis, Operations, and Navigation Toolkit Environment (Monte). We use the Rosetta mission data to validate the pipeline and obtain the spacecraft relative position with a 1-sigma covariance less than 3% of the radial distance, at 300 km from the body.*

Introduction. There is a growing interest in Small Body missions, which aim to advance the frontiers of science (as currently done by the OSIRIS-REx mission), In-Situ Resource Utilization and planetary defense (e.g. by the DART mission, which will study asteroids deflection in 2022). While approaching a Small Body, state-of-the-art relative navigation is currently based on a number of imaging techniques, such as Stereo Photoclinometry (SPC). While such techniques are crucial to fulfil mission requirements, e.g. following a target trajectory, they are also heavily dependent on ground support, where mission operators rely on human skill and intuition for recovering the shape, rotation and trajectory of the body. This results in higher mission complexity and cost and imposes potential limiting factors for advanced future operations, such as multi-agent exploration.

In this work, we present an optical-based strategy to perform autonomous navigation and mapping throughout the whole approach of a small celestial body, where we define the approach as the mission phase starting as soon as the Small Body is visible to the navigation camera and terminates when proximity operations start. During approach, the size of the body in the camera image continually increases, from a single pixel to the complete camera field of view. As shown in Figure 1, our strategy uses three phases to estimate the spacecraft orbit: periodicity (rotation rate of the small body) estimation, pole and shape estimation and precise orbit determination.

Orbit Determination Pipeline. Figure 2 shows a schematic of the full orbit determination pipeline: it starts from images as inputs, which are then processed to

estimate the body rotational kinematics and reference landmarks on the body’s surface. This set of parameters is used to define a dynamic model which, together with a camera model, is passed to the navigation filter. Finally, this navigation filter computes the spacecraft relative trajectory and refines the body’s kinematics. The following sections describe the estimation pipeline main steps.

Image Rendering. In order to generate images, which is needed to test the estimation pipeline, an image rendering tool is used. The simulator generates the picture captured from the spacecraft for a given time epoch, spacecraft-body relative trajectory and attitude, lighting conditions (i.e. direction of the Sun) and Small Body shape model. The whole scenario is generated based on state-of-the-art ephemeris and attitude data from the Rosetta mission (both from SPICE [4] kernels), the shape model of the Small Body, fed into a ray tracing-based image rendering engine (Blender Cycles). Figure 3 shows the comparison between real Rosetta mission images and simulated images.

Image Processing. Images are then processed to estimate the Small Body shape and kinematics as well as to estimate relative navigation parameters.

Rotation Rate Estimation. The spin rate of the Small Body can start to be estimated from early observations using standard light curve analysis: by processing the brightness time series of the images using a Fast-Fourier Transform to find the peak in the frequency spectrum. If we assume the Small Body to rotate about its principal axis only (i.e. a non-tumbling body), then the frequency peak represents twice its rotation rate.

Pole and Shape Model Estimation. Once the rotation rate is estimated, a Shape-from-Silhouette (SfS) algorithm [1] is used to extract both a shape model and the pole orientation. This routine leverages the high contrast between the black background and the body surface to extract the body silhouette. Then, the silhouette evolution over time is used to carve a cubic volume of voxels by removing those outside the silhouette limb. Finally, a Monte Carlo search is performed to estimate the best candidate pole orientation that minimizes the error between the predicted and observed silhouettes for each estimated shape model.

Feature Tracking. When the resolution suffices, visual features can start to be detected on the body’s surface and tracked from one image frame to another. We use Shi-Tomasi [2] corner features as detection method, and a Kanade-Lucas-Tomasi [3] approach for feature tracking. Dealing with features in the small body’s context

presents several challenges, such as dynamic lighting conditions, self-repetitive features and large scale-changes. In particular, features drift due to lighting changes have to especially be considered. Therefore, a tailored tuning for tracking and an outliers rejection method are implemented, to leverage a priori knowledge on the expected spacecraft-body relative dynamics. A feature tracking example is showed in Figure 4.

On-Surface Landmarks. To initialize relative navigation, observed visual features are projected onto the surface of the estimated body shape. A visual feature observed in the camera plane corresponds to a 3D landmark on the body's surface. A ray traces each visual feature from the camera plane through the camera's focal point and is intersected with the faces of the shape model generated by the Shape-from-Silhouette algorithm. The nearest intersection provides the 3D location of the corresponding landmark for the observed feature.

Monte Implementation. Image processing outputs are merged together to form one unique orbit determination solution. Astrodynamics and estimation tools included in JPL's Monte software are selected for this navigation filtering step in the pipeline.

Dynamics and Camera Model. In the estimation pipeline, a dynamics model and a camera model are used to predict optical measurements, given the current estimate of the relative trajectory and landmark locations. The dynamics model is defined by the Sun, main planetary bodies and target small body gravity, orbital maneuvers, stochastic accelerations and small body kinematics. The latter is provided by the image processing outputs (i.e. pole and rotation rate).

For each estimation step, both a predicted and an observed optical measurement are present, where one optical measurement is one feature in pixel coordinates. The residual between the two is computed for each feature and represents the navigation filter input.

Navigation Filter. A batch least-squares filter solves the estimation problem, given optical residuals and a dynamic model as inputs. We are interested in estimating a range of parameters in the filter: spacecraft relative trajectory, pole, rotation rate, landmarks location, comet gravity field and stochastic accelerations. To run the filter, though, we require initial estimates for each value, along with an *a priori* covariances. The optical residuals and dynamics model are then used with these initial estimates to provide the updated estimates for all parameters. One should note that no radiometric measurements are used in this estimation pipeline.

Approach Simulation. The estimation pipeline is validated by reproducing part of the Rosetta mission approach, seeded by real data in a realistic scenario in Monte. To date, the pipeline is based on two assumptions: the Small Body is assumed to rotate about its principal axis only and the spacecraft attitude is perfectly known at every time. The first assumption has

shown to be a good approximation for all the small bodies encountered to date. The second assumption is being removed in ongoing work.

Filter Setup. To simulate autonomous orbit determination, the filter is initialized with high *a priori* covariances. For example, the 1-sigma is 1000 km for the spacecraft position. The uncertainty on the small body ephemeris and scale is based on traditional ground-based uncertainties.

Results. We present here the orbit determination for a trajectory leg of the Rosetta approach. Simulation results are shown in Figure 5, expressed in the body-centered Radial-Transverse-Normal (RTN) frame [5]. The points in the plot represent the error between the estimated position value and the reference position (from SPICE kernels reconstructed trajectory) value, after each batch update. The error bars represent the related 1-sigma standard deviation. After about six hours, the radial position uncertainty drops to less approximately 10 km which, at roughly 300 km of radial distance, represents the 3% of radial error. Transverse and normal uncertainties are more than one order of magnitude smaller. Orbit determination performance are also shown in Figure 6, expressed into the equatorial plane of the comet-centered inertial frame.

Conclusions. The proposed solution, with less than 3% of global error in radial distance, holds promise for further development of an autonomous, optical-only-based, orbit-determination pipeline. We leverage Small Body images and dynamics knowledge of the environment to determine the relative trajectory and potentially propagate it in the future. Future work will focus on extending the simulation to all the approach phases, improving feature-tracking localization performance, including features description to enable loop closure capabilities and study the sensitivity of the filter to a priori information.

References.

- [1] S. Bandyopadhyay, I. Nesnas, S. Bhaskaran, B. Hockman, B. Morrell, "Silhouette-based 3D Shape Reconstruction of a Small Body from a Spacecraft", IEEE Aerospace Conference, Big Sky, MT, Mar. 2019.
- [2] J. Shi, C. Tomasi. "Good Features to Track", Computer Vision and Pattern Recognition, 593-600, 1994.
- [3] B. Lucas, T. Kanade "An Iterative Image Registration Technique with an Application to Stereo Vision", International Joint Conference on Artificial Intelligence, pages 674-679, 1981.
- [4] The Navigation and Ancillary Information Facility, SPICE data (SPICE kernels). Available at: <https://naif.jpl.nasa.gov/naif/data.html> (April 2019).
- [5] SMAP Spacecraft Frame Definitions Kernel. Available at: https://naif.jpl.nasa.gov/pub/naif/SMAP/kernels/fk/smap_pf_v14.tf

Acknowledgement: This research was carried out at the Jet Propulsion Laboratory, California Institute of Technology, under a contract with the National Aeronautics and Space Administration. © 2019 California Institute of Technology. All rights reserved.

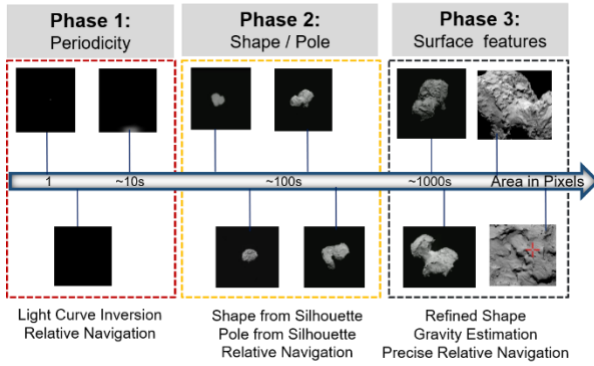


Figure 1. Phased approach schematic.

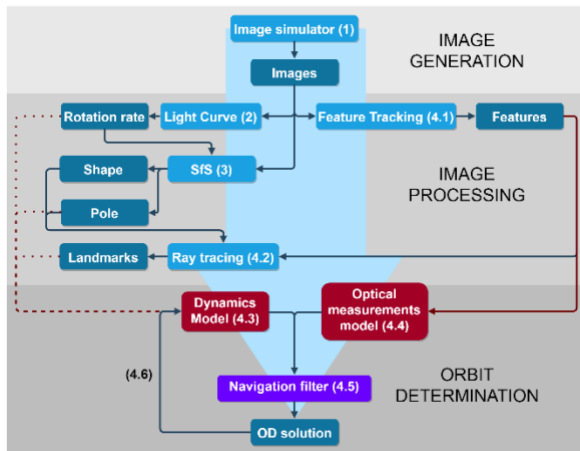


Figure 2. Orbit/rotation estimation pipeline.

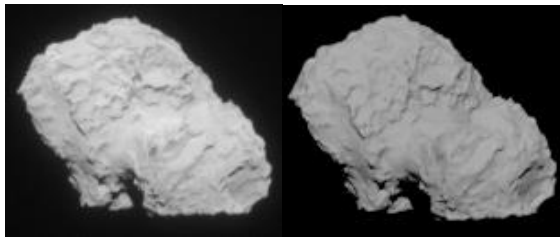


Figure 3. Comparison between real (left) image and simulated (right) image.

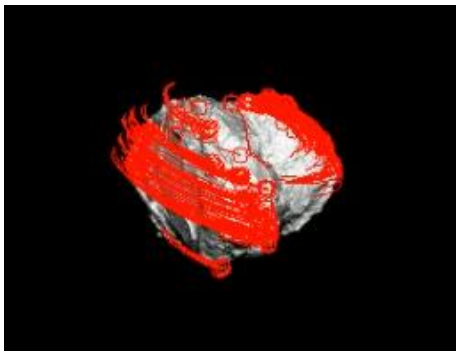


Figure 4. Feature tracking onto the camera Field of View: on-surface tracked features (red squares) and their paths in time (red lines). The same features are tracked on multiple images.

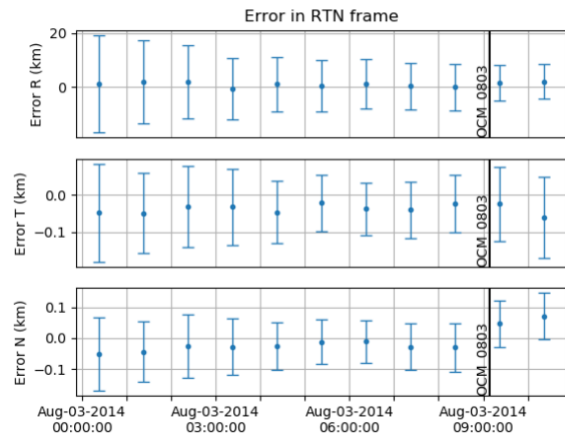


Figure 5. Error between estimated and reference trajectory in Radial-Transverse-Normal frame, at the end of the trajectory leg. The black vertical line represents the orbital control maneuver.

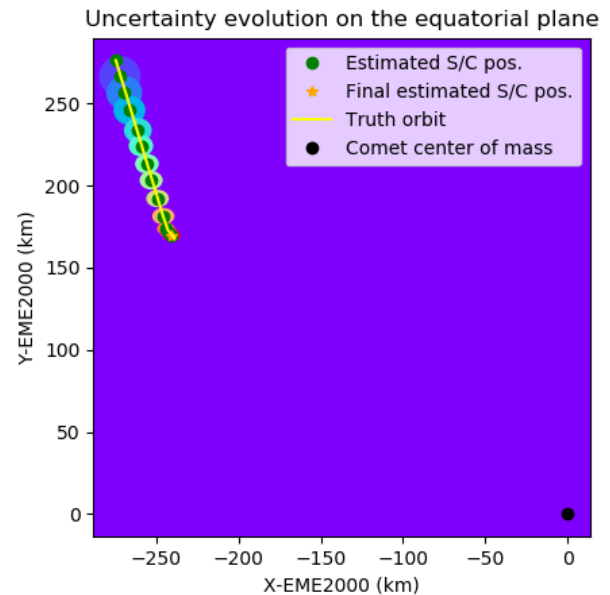


Figure 6. Trajectory estimation expressed onto the comet-centered EME2000 equatorial plane. Colored ellipses represent the 1-sigma bounds for each position update, evolving from cool colors to warm colors over time. The initial covariance (purple ellipse) is only partially included in this figure, as being orders of magnitude bigger.